MATERIALS SCIENCE

Ionoelastomer junctions between polymer networks of fixed anions and cations

Hyeong Jun Kim[1], Baohong Chen[2], Zhigang Suo[2]*, Ryan C. Hayward[1]*

Soft ionic conductors have enabled stretchable and transparent devices, but liquids in such devices tend to leak and evaporate. In this study, we demonstrate diodes and transistors using liquid-free ionoelastomers, in which either anions or cations are fixed to an elastomer network and the other ionic species are mobile. The junction of the two ionoelastomers of opposite polarity yields an ionic double layer, which is capable of rectifying and switching ionic currents without electrochemical reactions. The entropically driven depletion of mobile ions creates a junction of tough adhesion, and the stretchability of the junction enables electromechanical transduction.

Engineered devices for computation and signal propagation rely predominantly on electrons as charge carriers, whereas organisms primarily employ ions (*1*). This paradigm has begun to shift with the advent of ionotronic devices based on soft ionic conductors, such as hydrogels containing dissolved salts (*2*) or polymeric gels swollen by ionic liquids (*3*, *4*). These ionic conductors offer characteristics not easily accessible with electronic conductors, including intrinsic stretchability, optical transparency, and biocompatibility (*5*, *6*). Examples of such devices are transparent loudspeakers (*2*), stretchable touch pads (*7*), artificial axons (*8*), skin-like displays (*9*), and soft actuators (*10*, *11*).

The selective transport of holes and electrons in p- and n-type semiconductors, respectively, and the rectifying behavior of p-n junctions, provide the diodes, transistors, and logic elements that underly modern electronics (*12*). By analogy, ion pumps and selective ion channels allow for precise control of ion flow into and out of cell membranes, enabling sophisticated signal processing by nervous systems (*6*). Thus, the development of soft ionic analogs is expected to enable devices for computation, signal processing, and memory that are inherently deformable.

Efforts to rectify ionic currents within synthetic systems extend back 60 years to work by Lovrecek *et al.* (*13*) on aqueous solutions of high–molecular weight polyelectrolytes separated by a membrane. Later, bipolar membranes (*14*) and charged microchannels (*15*) were used to rectify and switch ionic currents, followed by applications in biosensors (*16*), logic gates (*17*), and power generators (*18*). More recently, solid-state ionic diodes (*19*, *20*) and transistors (*21*, *22*) have been demonstrated with the use of polyelectrolyte gels. These previous devices, however, suffer from key limitations inherent to liquid electrolytes, which can easily leak or evaporate. Moreover, they have exclusively relied on faradaic electrochemical processes to convert between ionic and electrical currents, limiting the signal response time by the electrochemical redox reaction rate (*19*) and complicating sustainable operation because of electrode dissolution, gas generation, and changes in chemical composition (*5*).

In this work, we demonstrate stretchable ionic devices using ionoelastomers, in which either anions or cations are fixed to an elastomer network but their counterions are mobile, making them ionic analogs of p- and n-type electronic semiconductors, respectively. A polyanion/polycation heterojunction leads to an ionic double layer (IDL), much like the depletion layer at a p-n semiconductor junction (Fig. 1A). By exploiting the wide electrochemical window of ionic liquid moieties, coupled with high–surface area carbon nanotube electrode/ionoelastomer interfaces, we demonstrate entirely non-faradaic rectification. This outcome enables stretchable ionic circuit elements, including diodes, transistors, and electromechanical transducers. The ionoelastomers consist entirely of cross-linked polyelectrolyte networks and associated

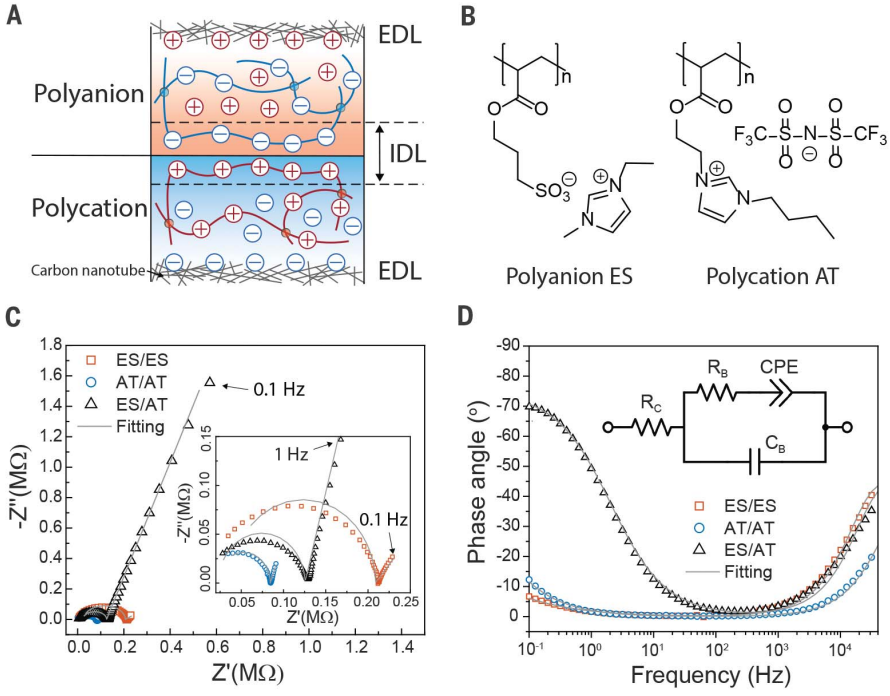

Fig. 1. Formation of an IDL at the interface of two oppositely charged ionoelastomers. (**A**) Schematic illustration of a polyanion/polycation junction. High–surface area carbon nanotube electrodes are embedded within each ionoelastomer, resulting in low-impedance (high-capacitance) EDLs. (**B**) Chemical structures of the polyanion ES and polycation AT. (**C**) Nyquist plot and (**D**) Bode phase plot of ac-impedance measurements. The inset in (C) shows an enlargement of the Nyquist plot in the low-impedance region. Gray lines represent fits of the equivalent circuit model shown in the inset of (D) to the ac-impedance data, where R_C, R_B, and C_B correspond to contact resistance, bulk resistance, and bulk polarization capacitance, respectively. A constant phase element (CPE) is used to describe the EDL (for ES/ES and AT/AT) or the IDL (for ES/AT). Z′, real part of complex impedance; Z″, imaginary part of complex impedance.

[1]Department of Polymer Science and Engineering, University of Massachusetts, Amherst, MA 01003, USA. [2]John A. Paulson School of Engineering and Applied Sciences, Kavli Institute for Bionano Science and Technology, Harvard University, Cambridge, MA 02138, USA.
*Corresponding author. Email: hayward@umass.edu (R.C.H.); suo@seas.harvard.edu (Z.S.)

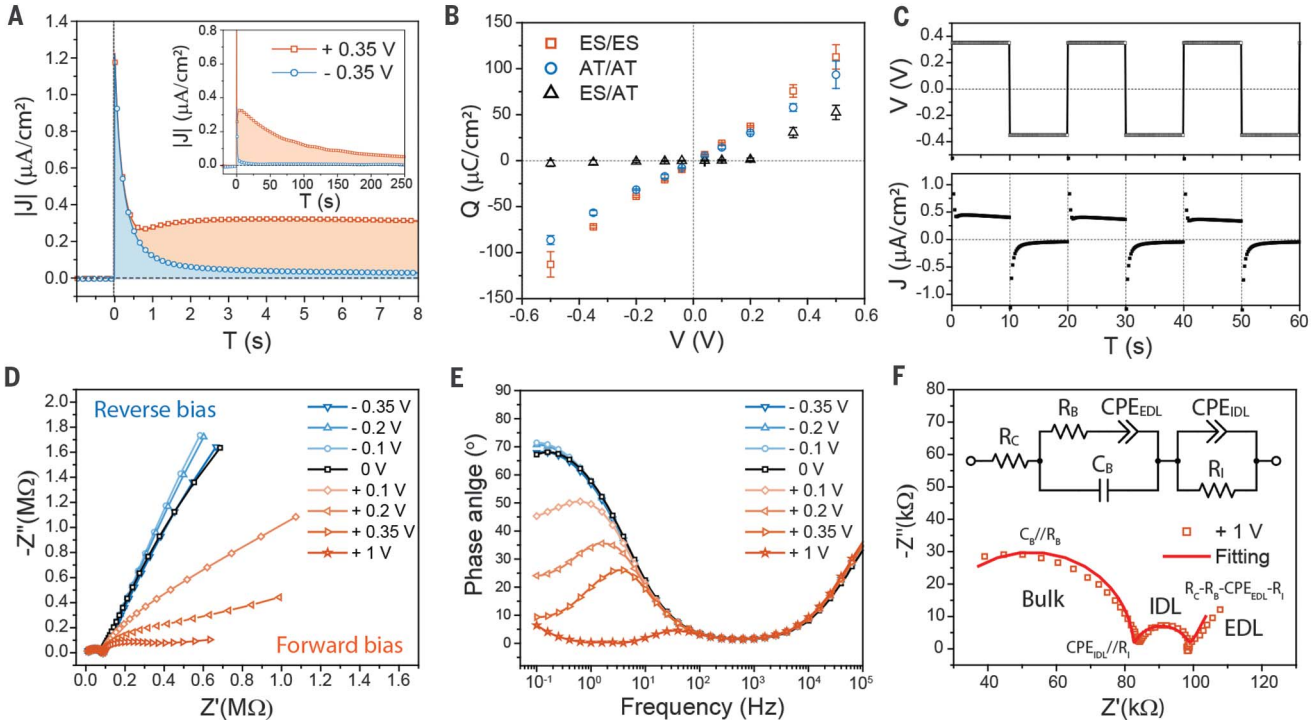

Fig. 2. Non-faradaic rectification by ionoelastomer diodes. (**A**) Current density of an ES/AT junction under a forward bias of +0.35 V and a reverse bias of −0.35 V, applied at 0 s. The inset shows a longer time period. (**B**) *Q-V* curves for ES/ES, AT/AT, and ES/AT. Error bars indicate SDs from more than five measurements for each point. (**C**) Rectification by ionoelastomer junctions under an alternating potential of ±0.35 V at 0.05 Hz. Applied voltage is plotted on the top; the corresponding current is shown on the bottom. (**D**) Nyquist plot and (**E**) Bode phase plot from ac-impedance measurements of ES/AT under dc biases. (**F**) Nyquist plot of ES/AT under +1 V. The equivalent circuit model for an ES/AT junction under dc bias is shown in the inset of (F). R_I, interfacial resistance.

counterions and contain no liquid components; thus, they are inherently not subject to leakage or evaporation.

We prepare polyanionic and polycationic ionoelastomers by polymerization of 1-ethyl-3-methyl imidazolium (3-sulfopropyl) acrylate (ES) and 1-[2-acryloyloxyethyl]-3-butylimidazolium bis(trifluoromethane) sulfonimide (AT), respectively (Fig. 1B), following modified literature procedures (*23*, *24*). The low glass transition temperatures (T_g) of these ionoelastomers enable selective ion conduction at ambient temperature by segmental motion of polymer chains (*25*). Lightly cross-linked ionoelastomers are highly stretchable [up to a uniaxial stretch ratio (λ_u) of 2.2], compatible with demands for flexible and wearable devices (*26*). In addition, whereas hydrogel devices rapidly lose water in ambient conditions and are challenging to seal, ionoelastomers are nonvolatile and have a wide electrochemical window (±~3 V) compared with polyelectrolyte hydrogels (<±1 V). Detailed experimental procedures and characterization of ionoelastomers are described in the supplementary materials (figs. S1 to S9).

After joining ES and AT ionoelastomers, mobile counterions near the interface diffuse into the opposite domain in a process driven by entropy. Excess fixed polyanionic and polycationic charges on the ES and AT sides, respectively, are left behind. Because the cross-linked networks do not permit long-range motion of the fixed ions, an interfacial electric field directed from AT to ES is developed, leading to a drift current of the mobile ions that exactly counterbalances their diffusion current at equilibrium (fig. S10), as described by extension of the classical model (*12*) of p-n semiconductors (see supplementary text for details).

The depletion of mobile ions and excess of fixed ions provides strong electrostatic adhesion between the two layers, such that peeling of an ES/AT junction leads to cohesive failure of the layers themselves with a toughness of G_c = 400 ± 24 J/m^2, whereas ES/ES and AT/AT homojunctions peel easily along the interface with $G_c \approx 40$ J/m^2 (fig. S11). In contrast to electronic semiconductor junctions, which typically require multistep lithographic fabrication processes, stretchable and robust ES/AT junctions can be easily prepared by attaching two preformed ionoelastomers.

We compare ES/ES and AT/AT homojunctions to ES/AT heterojunctions by ac-impedance measurements (Fig. 1, C and D). Impedance data are described using the equivalent circuit model in Fig. 1D (*27*), with fitted parameters in table S2. Capacitance values for ES/ES and AT/AT homojunctions are 150 ± 30 and 100 ± 20 μF/cm^2, respectively—roughly 100 times as large as the ~1 μF/cm^2 values typical of ionic liquid electrolytes with planar electrodes (*27*)—owing to the high surface areas of the carbon nanotube electrodes in our work. In stark contrast, the capacitance of an ES/AT heterojunction is 0.7 ± 0.2 μF/cm^2, clearly revealing the presence of the low-capacitance planar IDL at the ES/AT interface.

We characterize ionic rectification by applying dc biases of opposite signs to ES/AT heterojunctions. As shown in Fig. 2A, a forward bias voltage (V) of +0.35 V yields an exponential decay of current over a time (τ) of 71.0 ± 0.3 s, whereas a reverse bias of −0.35 V leads to a 200-fold more rapid decay (τ = 0.32 ± 0.01 s). The total associated charges (Q) by integrating these curves are 33 ± 5 and 0.7 ± 0.1 μC/cm^2, for + 0.35 V and −0.35 V, respectively. Full *Q-V* curves of all ionoelastomer junctions, summarized in Fig. 2B, show that ES/ES and AT/AT homojunctions have ideal linear capacitance curves ($C = Q/V$), with respective slopes of 220 and 170 μF/cm^2, of similar magnitude to the values from ac impedance. On the contrary, clear asymmetry is observed for

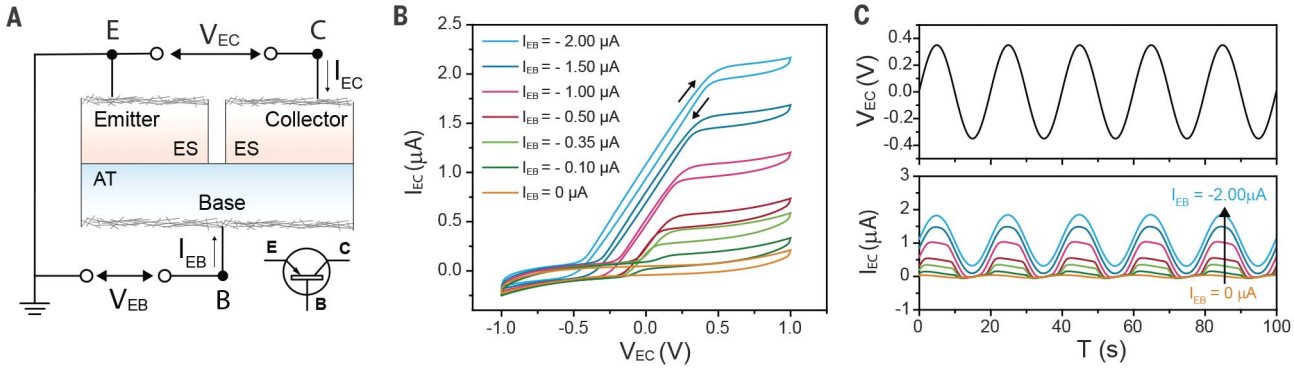

Fig. 3. Ionoelastomer transistor. (**A**) Device structure and circuit diagram of an ES/AT/ES ionoelastomer transistor connected in a common-emitter configuration. (**B**) Output characteristic (I_{EC}-V_{EC}) curves as a function of input current (I_{EB}). (**C**) Switching characteristics of an ES/AT/ES transistor under ac voltage of 0.35 V at 0.05 Hz.

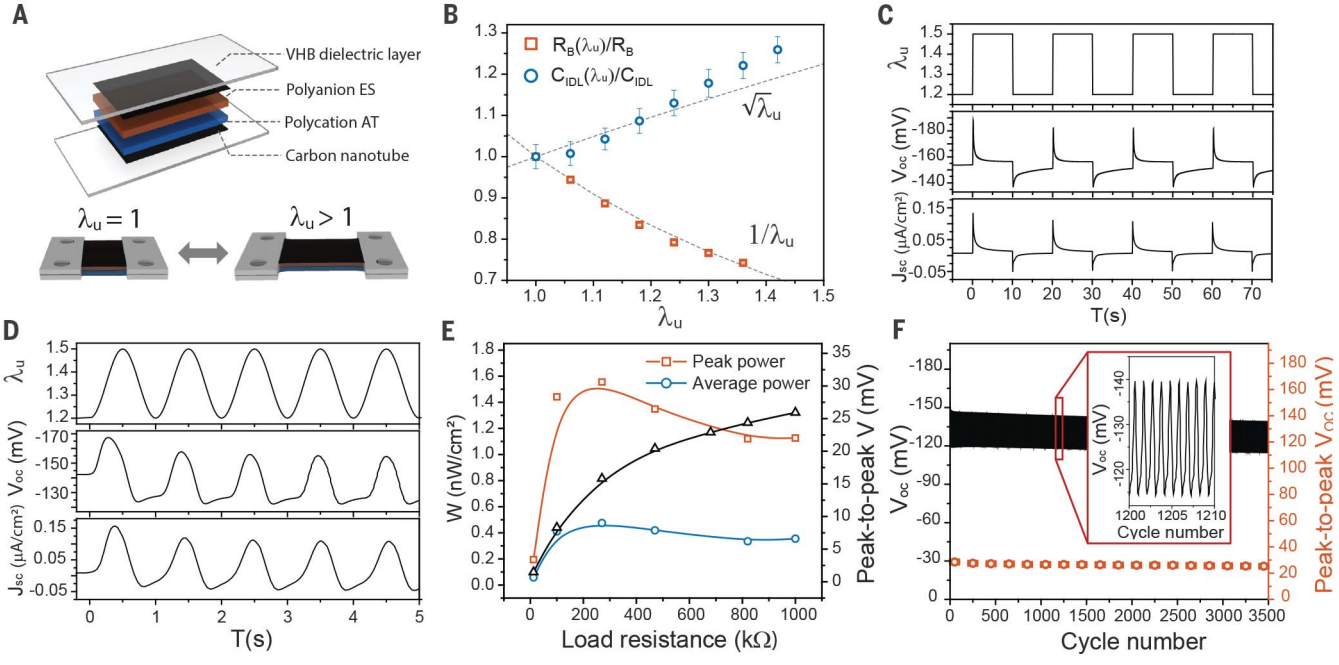

Fig. 4. Ionoelastomer electromechanical transducer. (**A**) Schematic illustration of an ES/AT electromechanical transducer. (**B**) Dependence of R_B and C_{IDL} on uniaxial stretch ratio λ_u. Cyclic uniaxial stretching from λ_u = 1.2 to 1.5 yields V_{oc} and J_{sc} under (**C**) 0.05-Hz square-wave strain and (**D**) 1-Hz sinusoidal strain. (**E**) Power (W) output under 1-Hz sinusoidal stretching as a function of load resistance. Optimized peak (red) and average (blue) W are achieved at 270 kilohms. (**F**) V_{oc} and peak-to-peak V_{oc} during 3500 cycles of operation at 1-Hz sinusoidal deformation.

ES/AT heterojunctions. The slope from −0.5 to +0.2 V is 2.1 ± 0.2 μF/cm^2, comparable to the IDL capacitance from ac impedance, whereas from +0.2 to +0.5 V the slope increases substantially to 170 μF/cm^2, characteristic of a high–surface area electric double layer (EDL) capacitance.

When a reverse bias is applied to ES/AT junctions, mobile ions are pulled away from the interface, charging the IDL capacitor, with a correspondingly short resistor-capacitor time (τ_{RC}) and small Q due to its low capacitance. Under forward bias, however, mobile ions are pushed from ES to AT and vice versa; once the bias exceeds the built-in potential of ≈0.2 V, the IDL is destroyed and the interface behaves resistively. Then, the ES/AT circuit effectively contains only the high-capacitance EDLs, resulting in an increase in τ_{RC} and Q by roughly two orders of magnitude. Exploiting this asymmetry, we demonstrate a rectifying solid-state ionic diode based on non-faradaic processes (Fig. 2C). The rectification ratio (Q_f/Q_r, where Q_f and Q_r respectively denote the charge at forward and reverse bias) at ±0.35 V is 50, comparable to the ratio for previously reported faradaic ionic diode systems (I_f/I_r ≈ 2 to 40, where I_f and I_r respectively denote the current at forward and reverse bias) (*20*, *28*). Moreover, the rectification ratio of ionoelastomer diodes can readily be tuned by the capacitance asymmetry of the EDL and IDL, enabling an increase to 550 by using microporous carbon electrodes with EDL capacitance an order of magnitude higher than that of the IDL (fig. S12). This quality, coupled with their soft, elastic, and liquid-free nature, makes such ionoelastomer diodes highly attractive

as components for controlling ionic currents in integrated circuits, soft actuators, energy conversion and storage applications, and wearable or implantable devices.

A more detailed explanation of the diode behavior is provided by ac impedance of ES/AT junctions under dc biases in Fig. 2, D to F. To capture the IDL response to applied bias, we develop an equivalent circuit model (Fig. 2F, inset; see supplementary text for details) containing elements that represent the interfacial capacitance (CPE_{IDL}) and resistance (R_I). With increasing forward bias, R_I rapidly decreases as mobile ions accumulate at the interface to destroy the IDL (fig. S13). This reduction in interfacial resistance results in decreased low-frequency (<100 Hz) impedance (red line in Fig. 2D) and a pronounced decrease in the low-frequency peak in phase angle corresponding to the IDL capacitance (Fig. 2E).

We next fabricate an ES/AT/ES ionoelastomer transistor (Fig. 3A). Two ES layers serve as the emitter (E) and collector (C), and an AT layer serves as the base (B). We ground the emitter, supply the emitter-base input current (I_{EB}), and record the emitter-collector output characteristic curves (I_{EC}-V_{EC}) on the basis of cyclic potential sweeps from –1 V to 1 V at 0.1 V/s (Fig. 3B). When I_{EB} = 0, either the E/B or C/B interface is always under reverse bias during the sweep of V_{EC}, leading to a small I_{EC} limited by the IDL capacitance. However, with negative I_{EB}, mobile anions in AT are pushed to the E/B and C/B interfaces, destroying the IDLs and enabling a regime of linear resistive I_{EC}-V_{EC} curves. On the basis of the output characteristics (full data in fig. S14), we demonstrate switching of non-faradaic ac currents (Fig. 3C). The ratio of root mean square currents between the on ($I_{EB} \leq -1\ \mu A$) and off ($I_{EB} \geq 0\ \mu A$) states is measured to be ≈40, comparable to values of 35 to 100 for polyelectrolyte hydrogel transistors (*21*, *22*). Again, however, this value is limited by the electrode capacitance and can be improved to ≈150 with the use of microporous carbon electrodes (fig. S15). In addition to the ability of the ionoelastomer transistor to function under uniaxial stretching up to λ_u = 1.6 (fig. S16), its non-faradaic and liquid-free nature offer a critical step toward ionic logic devices with robust and long-term sustained operation.

A distinctive advantage of ionoelastomer devices is that they are elastic and deformable. As shown in Fig. 4A, an ES/AT junction is uniaxially stretched to λ_u times its initial length, and the corresponding changes in bulk resistance (R_B) and capacitance of IDL (C_{IDL}) are measured using ac impedance (fig. S17). Assuming that both materials are incompressible, the resistance should decrease as $1/\lambda_u$, owing to the decrease in thickness and increase in in-plane area by $\sqrt{\lambda_u}$, whereas the latter effect should provide a corresponding increase in C_{IDL}. Both expectations are in agreement with the measurements in Fig. 4B. Stretching of ES/ES and AT/AT homojunctions (fig. S18) yields a decrease in R_B that is consistent with the expected $1/\lambda_u$ dependence, whereas the EDL capacitances remain nearly constant because the rigid carbon nanotubes are simply realigned along the stretching direction and the true contact area with the soft ionoelastomer matrix is unchanged.

Deformation of ES/AT junctions leads to an electrical response, enabling the transduction of mechanical movements into electrical signals for sensing and energy harvesting. We monitor the open-circuit voltage (V_{oc}) and short-circuit current density (J_{sc}) of ES/AT junctions under cyclic uniaxial stretching from λ_u = 1.2 to 1.5 (0.05-Hz square-wave profile in Fig. 4C). From one cycle of stretching, a peak-to-peak V_{oc} of 46 ± 2 mV and a peak-to-peak J_{sc} of 0.18 ± 0.01 $\mu A/cm^2$ are generated (see fig. S19 for additional data). Similarly, the electrical response under sinusoidal deformation at 1 Hz (Fig. 4D) yields ΔV_{oc} = 37 ± 3 mV and ΔJ_{sc} = 0.20 ± 0.05 $\mu A/cm^2$ (table S4). Meanwhile, ES/ES and AT/AT homojunctions showed negligible responses (ΔV_{oc} < 1 mV and ΔJ_{sc} < 5 nA/cm^2) for the same conditions (fig. S20), revealing the key role of the IDL in the electromechanical response of ES/AT junctions.

The power (W) generated by deforming ES/AT junctions is shown in Fig. 4E as a function of load resistance, with an optimum value of W = 1.6 nW/cm^2 at 270 kilohms for sinusoidal stretching at 1 Hz. This operating frequency is well matched with ambient mechanical sources (fig. S21) such as ocean waves, wind, and human motion, whereas most existing mechanical energy harvesters, including piezoelectrics and ferroelectrics, are inherently limited at <5 Hz (*29*, *30*). In addition, power generation from ES/AT is stable over at least 3500 cycles (Fig. 4F). Although the power output must be improved by several orders of magnitude to be competitive with that of existing technologies, the electrical response of only a thin interfacial layer is currently used for energy harvesting.

An ionoelastomer heterojunction exhibits entropic depletion of mobile ions, forms an ionic double layer, and adheres spontaneously with high toughness. By using high–surface area carbon nanotube electrodes, we demonstrate liquid-free ionoelastomer diodes, transistors, and electromechanical transducers based on capacitive non-faradaic processes. Nature offers only one species of electron but numerous species of ion, which may soon translate to ionoelastomer devices with a wide range of physicochemical and biological activities.

REFERENCES AND NOTES

1. C. Yang, Z. Suo, *Nat. Rev. Mater.* **3**, 125–142 (2018).
2. C. Keplinger *et al.*, *Science* **341**, 984–987 (2013).
3. B. Chen *et al.*, *ACS Appl. Mater. Interfaces* **6**, 7840–7845 (2014).
4. Y. Hou *et al.*, *Adv. Energy Mater.* **7**, 1601983 (2017).
5. H.-R. Lee, C.-C. Kim, J.-Y. Sun, *Adv. Mater.* **30**, e1704403 (2018).
6. H. Chun, T. D. Chung, *Annu. Rev. Anal. Chem.* **8**, 441–462 (2015).
7. C.-C. Kim, H.-H. Lee, K. H. Oh, J.-Y. Sun, *Science* **353**, 682–687 (2016).
8. C. H. Yang *et al.*, *Extreme Mech. Lett.* **3**, 59–65 (2015).
9. C. Larson *et al.*, *Science* **351**, 1071–1074 (2016).
10. O. Kim, S. J. Kim, M. J. Park, *Chem. Commun.* **54**, 4895–4904 (2018).
11. T. Li *et al.*, *Sci. Adv.* **3**, e1602045 (2017).
12. B. G. Streetman, *Solid State Electronic Devices* (Prentice Hall, 1990).
13. B. Lovrecek, A. Despic, J. O. M. Bockris, *J. Phys. Chem.* **63**, 750–751 (1959).
14. S. Mafé, P. Ramírez, *Acta Polym.* **48**, 234–250 (1997).
15. B. Yameen *et al.*, *J. Am. Chem. Soc.* **131**, 2070–2071 (2009).
16. I. Vlassiouk, T. R. Kozel, Z. S. Siwy, *J. Am. Chem. Soc.* **131**, 8211–8220 (2009).
17. J.-H. Han, K. B. Kim, H. C. Kim, T. D. Chung, *Angew. Chem. Int. Ed.* **48**, 3830–3833 (2009).
18. T. B. H. Schroeder *et al.*, *Nature* **552**, 214–218 (2017).
19. O. J. Cayre, S. T. Chang, O. D. Velev, *J. Am. Chem. Soc.* **129**, 10801–10806 (2007).
20. H.-R. Lee *et al.*, *Adv. Funct. Mater.* **29**, 1806909 (2018).
21. K. Tybrandt, R. Forchheimer, M. Berggren, *Nat. Commun.* **3**, 871 (2012).
22. K. Tybrandt, K. C. Larsson, A. Richter-Dahlfors, M. Berggren, *Proc. Natl. Acad. Sci. U.S.A.* **107**, 9929–9932 (2010).
23. A. S. Shaplov *et al.*, *Macromolecules* **44**, 9792–9803 (2011).
24. H. Chen, J.-H. Choi, D. Salas-de la Cruz, K. I. Winey, Y. A. Elabd, *Macromolecules* **42**, 4809–4816 (2009).
25. F. Fan *et al.*, *Macromolecules* **49**, 4557–4570 (2016).
26. J. A. Rogers, T. Someya, Y. Huang, *Science* **327**, 1603–1607 (2010).
27. J.-H. Choi, W. Xie, Y. Gu, C. D. Frisbie, T. P. Lodge, *ACS Appl. Mater. Interfaces* **7**, 7294–7302 (2015).
28. Y. Wang, Z. Wang, Z. Su, S. Cai, *Extreme Mech. Lett.* **28**, 81–86 (2019).
29. M. Lallart, P.-J. Cottinet, D. Guyomar, L. Lebrun, *J. Polym. Sci. B* **50**, 523–535 (2012).
30. S. H. Kim *et al.*, *Science* **357**, 773–778 (2017).
31. H. Kim, B. Chen, Z. Suo, R. C. Hayward, Ionoelastomer Junctions Between Polymer Networks of Fixed Anions and Cations, 104, Data and Datasets, ScholarWorks at UMass Amherst (2019); https://doi.org/10.7275/k23d-6081.

ACKNOWLEDGMENTS

Funding: This work was supported by the National Science Foundation through grant DMR-1609972 (R.C.H. and H.J.K.) and the NSF MRSEC at Harvard through grant DMR-1420570 (Z.S. and B.C.). **Author contributions:** R.C.H. and Z.S. supervised the project. H.J.K. and B.C. designed the experiments, solved the technical issues, and checked the experimental results. All authors contributed to developing the concept, interpreting the results, and preparing the manuscript. **Competing interests:** The authors declare no competing interests. **Data and materials availability:** All data have been deposited in the ScholarWorks at UMass Amherst database (*31*).

SUPPLEMENTARY MATERIALS

science.sciencemag.org/content/367/6479/773/suppl/DC1
Materials and Methods
Supplementary Text
Figs. S1 to S21
Tables S1 to S4
References (*32*–*39*)

24 July 2019; accepted 6 January 2020
10.1126/science.aay8467

Ionoelastomer junctions between polymer networks of fixed anions and cations

Hyeong Jun Kim, Baohong Chen, Zhigang Suo and Ryan C. Hayward

Science **367** (6479), 773-776.
DOI: 10.1126/science.aay8467

Ionic elastomeric material electronics

Wearable devices often need to be soft or flexible, and ideally, these properties would extend beyond packaging material to also include the electronics. Some soft ionic conductors have been made in the form of flexible, stretchable, and transparent devices, but leaks from these materials is a concern. Kim *et al.* demonstrate ionic elastomeric diodes and transistors that harness ionic double layers to rectify and switch ionic currents (see the Perspective by Gao and Lee). This is achieved without trapped liquids by fixing the anions or cations to an elastomer network while the other species of ions remain mobile.

Science, this issue p. 773; see also p. 735

Science (print ISSN 0036-8075; online ISSN 1095-9203) is published by the American Association for the Advancement of Science, 1200 New York Avenue NW, Washington, DC 20005. The title *Science* is a registered trademark of AAAS.